Dyes and Pigments 85 (2010) 43–50

Contents lists available at ScienceDirect

Dyes and Pigments

journal homepage: www.elsevier.com/locate/dyepig

1-(Carbamoylmethyl)-3*H*-indolium squaraine dyes: Synthesis, spectra, photo-stability and association with BSA

Bingshuai Wang, Jiangli Fan, Shiguo Sun, Li Wang, Bo Song, Xiaojun Peng*

State Key Laboratory of Fine Chemicals, Dalian University of Technology, 158 Zhongshan Road, Dalian 116012, PR China

ARTICLE INFO

Article history:
Received 6 July 2009
Received in revised form
1 October 2009
Accepted 2 October 2009
Available online 28 October 2009

Keywords:
Squarylium dye
Aggregation
Photo-stability
Fluorescence
Bovine serum albumin
Linear relationship

ABSTRACT

Novel, squarylium dyes containing 1-(alkylcarbamoylmethyl)-2,3,3-trimethyl- 3*H*-indolium groups were synthesized and their UV/Vis and fluorescence spectra, aggregation, photo-stability and association with bovine serum albumin were studied. The absorption and emission max wavelengths of the dyes in different solvents were in the range 619–653 nm. Compared to a typical ethyl squarylium dye, the introduction of alkylcarbamoylmethyl groups reduced aggregation and improved molar extinction coefficient, fluorescence quantum yield and photo-stability in water. Moreover, the fluorescence intensity of the dyes increased upon the addition of BSA in pH 7.0 phosphate buffer solution. An excellent linear relationship (r^2 = 0.9982) was obtained between fluorescence intensity and bovine serum albumin concentration.

1. Introduction

Squaraine dyes possess good photoconductivity [1], high extinction coefficient [2], and intense fluorescence [3]. These features make them useful in a variety of applications such as photoconductive materials [4], organic solar cells [5] and optical discs [6]. The dyes also enjoy use as long-wavelength fluorescent probes and labels in biological assay, since their absorption and fluorescence spectra lie in the visible red and near-infrared regions (NIR), which are outside the self-absorption and self-luminescence regions of biological objects [7,8].

Squarylium dyes derived from 2,3,3-trimethyl-3*H*-indolium and its derivatives are important as some of these dyes (such as **I** and **II** in Fig. 1) have been used as non-covalent protein probes of high fluorescence intensity [7,9,10]; however, the dyes display poor photo-stability and low water-solubility. To improve the photo-stability of squarylium dyes, much effort has been devoted to molecular structure adjustment of the benzene ring of the indolinium salt. The introduction of an electron-withdrawing groups such as chloro and nitro affords considerable protection against fading [11,12]. Recently, the present authors found that electron-withdrawing groups on the *N*-benzyl group of **III** (Y = CO_2H or NO_2 in Fig. 1) improved photo-stability markedly [13]. In contrast, the water-solubility of fluorescent probes is a significant issue in biological applications; whilst the introduction of charged groups such as sulfonate (**III**, **IV** in Fig. 1) into the dyes can increase water-solubility, that accompanying ionic charge can lower the dye's binding potency [14]. Although some progresses had been achieved through the introduction of nonionic groups into polymethine cyanine dyes [15,16], the improvement in squaraine dyes has been limited.

This paper concerns novel 2,3,3-trimethyl-3*H*-indolium squaraine dyes that contain alkylcarbamoylmethyl groups (Fig. 2) and the effects which the moderate nonionic hydrophilicity and high electron-withdrawing ability of such groups have, upon the water-solubility and photo-stability of squarylium dyes.

2. Experiments

2.1. Materials and general methods

Deionized water was redistilled before use. Other chemicals used for the experiments were of analytical grade. Mass spectral determinations were made on HP1100 API-ES mass spectrometry. ^{1}H NMR spectra were recorded on a Varian 400 MHz NMR spectrometer. Fluorescence measurements were performed on a PTI-C-700 Felix and Time-Master system. Visible spectra were measured on an HP-8453 spectrophotometer.

* Corresponding author. Tel.: +86 0411 39893899; fax: +86 0411 39893800.
E-mail address: pengxj@dlut.edu.cn (X. Peng).

0143-7208/$ – see front matter © 2009 Elsevier Ltd. All rights reserved.
doi:10.1016/j.dyepig.2009.10.002

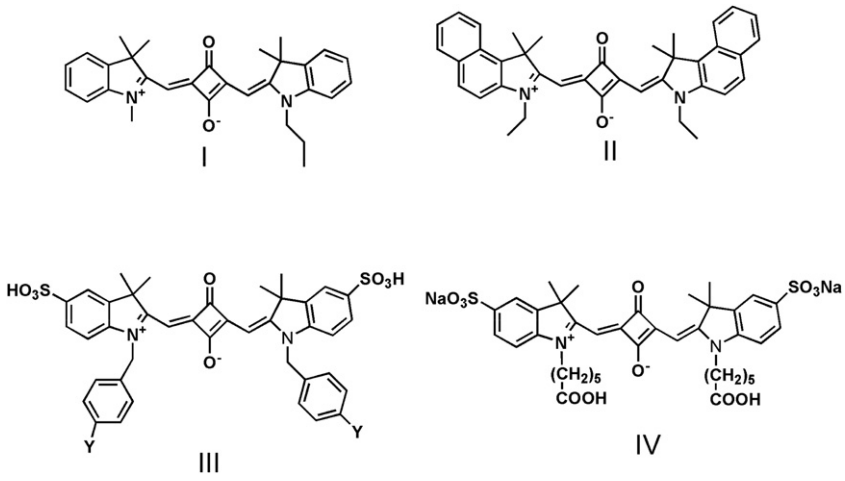

Fig. 1. Squarylium dyes from 2,3,3-trimethyl-3*H*-indolium.

2.2. Determination of quantum yield

The relative fluorescence quantum yields were determined by using Rhodamine B ($\phi = 0.56$ in ethanol) as standard [17] and were calculated through the following equation [18]:

$$\Phi_x = \Phi_s(F_x/F_s)(A_x/A_s)(\lambda ex_s/\lambda ex_x)(n_x/n_s)^2$$

where Φ = quantum yield; F = integrated area under the corrected emission spectrum (in Ep units); A = absorbance at the excitation wavelength; λex = the excitation wavelength; n = the refractive index of the solution (because of the low concentrations of the solutions (10^{-7}–10^{-8} mol/L), the refractive indices of the solutions are replaced with those of the solvents.); and the subscripts x and s refer to the unknown and the standard, respectively.

2.3. Aggregation

The absorption spectra display no obvious change when the concentrations of the dye solutions are lower than 1 μM. Otherwise, when the concentration is higher than 40 μM, the dyes tend to deposit from the solutions. So 1–40 μM were chosen as the testing concentration ranges for all dyes except dye **3b**. The absorption density of dye **3b** solution would exceed the maximum limit (<3) of the absorption instrument in high concentrations (>20 μM), so **3b** was kept in 1–20 μM. The formation of aggregation leads to a change in the wavelength maxima and shape of the absorption band which can be used to recognize the occurrence of aggregation. The absorption intensity is proportional to the concentrations of the dyes in low concentration, but the aggregation will make the absorption density of the monomer decrease, so the spectra are normalized (each spectrum data divided by its maximum absorption value) in order to facilitate direct comparisons on the shapes of the spectra. The loss of monomer absorption density in higher concentrations relative to 1 μM can indicate the relative amount of aggregated molecules.

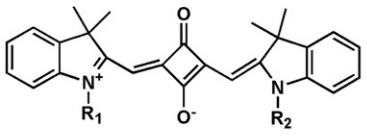

3b: $R_1=R_2=CH_2CON(C_2H_5)_2$, **3b$_1$**: $R_1=CH_3$, $R_2=CH_2CON(C_2H_5)_2$,

3c$_1$: $R_1=CH_3$, $R_2=CH_2CONH(n\text{-}Pr)$,

Fig. 2. Structures of 2,3,3-trimethyl-3*H*-indolium squaraine dyes.

2.4. Photo-stability

The photo-stability tests were carried out in quartz cells (10 mm in width) where sample solutions were irradiated with a 500 W Iodine-tungsten (I/W) lamp at room temperature. The distance between the cells and the lamp was 350 mm. The 5 μM solutions of the dyes in CH_3CN were radiated and the irreversible bleaching of the dyes at the absorption peak was monitored as a function of time.

2.5. Redox potential

The redox potential was measured on BAS 100B electorchemical analyser. A three- electrode cell was composed of a glass carbon as working electrode, a platinum wire as counter electrode, and Ag/Ag^+as reference electrode (0.01 M $AgNO_3$). The supporting electrolyte was $TBAPF_6$ (0.1 M tetra n-butylammonium hexafluorophosphate) and the concentrations of the dyes were 10^{-3} M in CH_3CN.

2.6. Dye–BSA association

The association of 2 μM dye (3a, 3b, III) and 100 μM BSA was conducted in order to ascertain the association time. The fluorescence-time curves were presented in Fig. 3 and which shows the

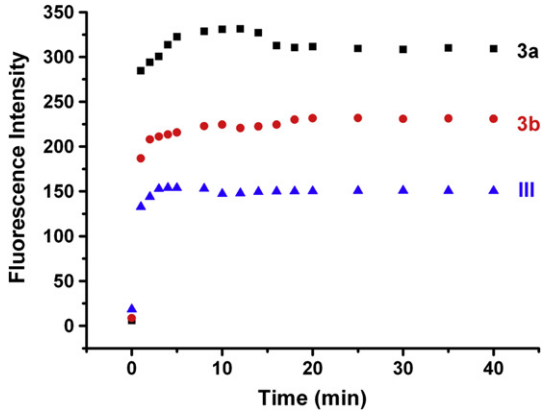

Fig. 3. The time-dependence curves of dye 3a (black line), 3b (red line) and III (blue line) associated with 100 μM BSA.

fluorescence intensities of the dyes reach the balance after 20 min, so the association time of 20 min was chosen.

The concentrations of the dyes were kept constant at 2 μM. After BSA was added for 20 min, the fluorescence spectra of the dyes were recorded with increasing the BSA concentration until the fluorescence intensity of dye–BSA become saturated in pH = 7.0 phosphate buffer solution (PBS). Dye–BSA associations in different pH buffer solutions were also studied in order to compare the effect of pH.

2.7. Synthesis

The synthetic routes of the dyes are shown in Fig. 4. Indolium quaternized salts **2a** and **2e** were synthesized according to the literature procedure [19]. To serve as a reference, the well-known squarylium dye **3a** (R = CH_2CH_3) was also synthesized. Yield: 75%. Dye **3a**: ^{1}H NMR(400 MHz, Acetone-d6, ppm): δ1.36 (t, 6H, *J* = 7.2 Hz, CH_3CH_2), 1.74 (s, 12H, C(CH_3)$_2$), 4.18 (q, 4H, CH_3CH_2), 5.88 (s, 2H, *CH*), 7.15 (t, 2H, *J* = 7.6 Hz, Ar-*H*), 7.25 (d, 2H, *J* = 8.0 Hz, Ar-*H*), 7.34 (t, 2H, *J* = 8.0 Hz, Ar-*H*), 7.47 (d, 2H, *J* = 7.6 Hz, Ar-*H*). ESI-MS, *m*/*z*: 453.3 $[M + H]^+$.

2.7.1. Synthesis of intermediates 1b and 1c

A chloroform solution (10 mL) of 2-chloroacetyl chloride (4.52 g, 40 mmol) was added dropwise to a chloroform (10 mL) solution of appropriate alkyl amine (40 mmol) with stirring at 0–10 °C, then the solution was heated to reflux for 2 h, the solvent was removed by a rotary evaporator to get the chloromethylamides as yellow liquids.

2.7.2. General procedure for the synthesis of indolium quaternized salts 2b, 2c and 2d

2,3,3-Trimethyl-3*H*-indolenine (3.20 g, 20 mmol) and appropriate halide (40 mmol) were mixed in toluene (15 mL) under nitrogen in 50 mL flask and refluxed for 24–48 h until the solid appeared around the flask. The ensuing mixture was cooled to room temperature and added to diethyl ether (100 mL); the precipitate was filtered and washed with ethyl acetate (20 mL × 3). The corresponding compound was used in the next reaction without further purification. The following indolium quaternized salts were prepared:

1-(*N*, *N*-diethylacetamide-2-yl) −2, 3, 3-trimethyl-3*H*-indolium quaternized salt (chloride) **2b**. Reaction time: 48 h; Yield: 52%; Red powder. 1-(*N*-propylacetamide-2-yl)-2, 3, 3-trimethyl-3*H*-indolium quaternized salt (chloride) **2c**. Reaction time: 48 h; Yield: 41%; Red powder.

1-(methyl acetate-2-yl)-2, 3, 3-trimethyl-3*H*-indolium quaternized salt (bromide) **2d**. Reaction time: 24 h; Yield: 56%; Fawn powder.

2.7.3. Synthesis of dyes 3a–3e

*2.7.3.1. Dye **3b**.* Squaric acid (114 mg, 1 mmol) was heated under reflux in a mixture of toluene (10 mL) and n-butanol (10 mL). Upon dissolution of the squaric acid, a pyridine (5 mL) solution of **2b** (680 mg, 2.2 mmol) was added and, after refluxing for 3 h, the reaction mixture was cooled to room temperature and the solvents were removed by rotary evaporation. The residue was treated with diethyl ether (100 mL) and the precipitate was filtered. Further purification was achieved using column chromatography emplying ethyl acetate-acetone mixture as eluent. When the solvents were removed, a blue solid powder was obtained which was recrystallized from acetone, providing bright green crystals (248 mg) collected in 40% yield. ^{1}H NMR (400 MHz, $CDCl_3$, ppm): δ1.14 (t, 6H, *J* = 6.8 Hz, CH_3CH_2), 1.38 (t, 6H, *J* = 6.8 Hz, CH_3CH_2), 1.739 (s, 12H, C(CH_3)$_2$), 3.42 (q, 4H, CH_3CH_2), 3.51 (q, 4H, CH_3CH_2), 5.09 (s, 4H, CH_2–N), 5.75 (s, 2H, C–*CH*═C), 6.79 (d, 2H, *J* = 7.6 Hz, Ar-*H*), 7.13 (t, 2H, *J* = 7.6 Hz, Ar-*H*), 7.26 (t, 2H, *J* = 7.6 Hz, Ar-*H*), 7.33 (d, 2H, *J* = 7.6 Hz, Ar-*H*). ESI-MS, *m*/*z*: 623.3 $[M + H]^+$.

*2.7.3.2. Dye **3b$_1$**.* Squaric acid (114 mg, 1 mmol) was heated under reflux in a mixture of toluene (10 mL) and n-butanol (10 mL). Upon dissolution of the squaric acid, a pyridine (5 mL) solution of intermediate **2e** (301 mg, 1 mmol) was added. After refluxing for 0.5 h, a further pyridine (5 mL) solution of intermediate **2b** (371 mg, 1.2 mmol) was added. After refluxing for 3 h, the reaction mixture was cooled to room temperature and the solvent removed by rotary evaporation. The residue was treated with diethyl ether (100 mL) and the resulting precipitate was filtered. Further purification was achieved using column chromatography emplying ethyl acetate-acetone mixture as eluent. The solvents were removed and a lue solid powder (225 mg) was obtained in 43% yield. ^{1}H NMR (400 MHz, Acetone-d6, ppm): δ1.07 (t, 6H, *J* = 6.8 Hz, CH_3CH_2), 1.39 (t, 6H, *J* = 6.8 Hz, CH_3CH_2), 1.72 (s, 6H, C(CH_3)$_2$), 1.75 (s, 6H, C(CH_3)$_2$), 3.38 (q, 2H, CH_3CH_2), 3.63 (s, 3H, CH_3–N), 3.64 (q, 2H, CH_3CH_2), 5.12 (s, 2H, CH_2–N), 5.70 (s, 1H, C–*CH*═C), 5.84 (s, 1H, C–*CH*═C), 7.06 (d, 1H, *J* = 7.6 Hz, Ar-*H*), 7.13 (m, 2H, Ar-*H*), 7.25 (m, 2H, Ar-*H*), 7.33 (t, 1H, *J* = 7.6 Hz, Ar-H), 7.44 (d, 2H, *J* = 7.2 Hz, Ar-H). ESI-MS, *m*/*z*: 524.3 $[M + H]^+$.

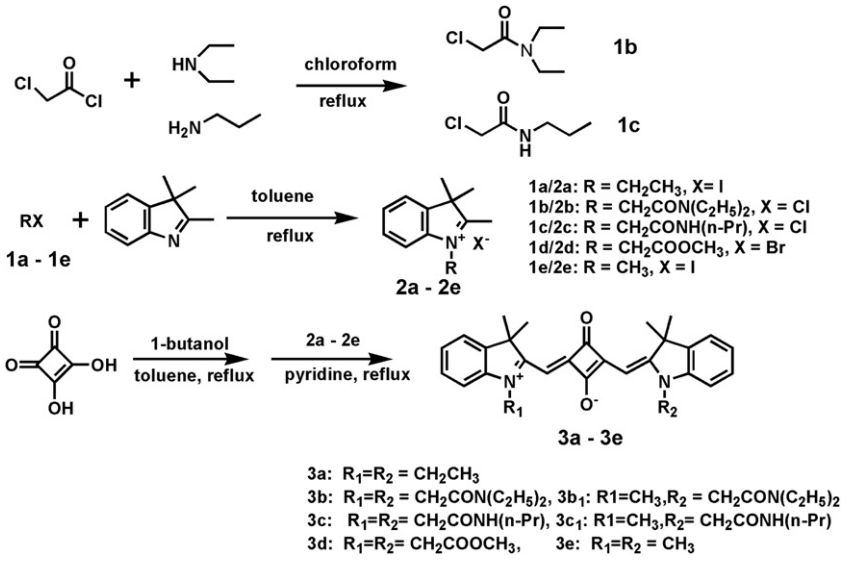

Fig. 4. Synthesis of the squarylium dyes.

*2.7.3.3. Dye **3c**.* The syntheses and purification of **3c** were the same as that of **3b**. However, analyzing the MS and ^{1}H NMR of the compound, we found the crystal was not our target compound **3c** but **3c$_1$**. The reason was discussed in the part 3.

Yield: 25 %. ^{1}H NMR (400 MHz, $CDCl_3$, ppm): δ0.84 ((t, 3H, J = 7.6 Hz, $CH_3CH_2CH_2$), 1.47 (m, 2H, $CH_3CH_2CH_2$), 1.69 (s, 6H, C(CH_3)$_2$), 1.77 (s, 6H, C(CH_3)$_2$), 3.21 (q, 2H, $CH_3CH_2CH_2$), 3.49 (s, 2H, CH_2–N), 3.64 (s, 3H, CH_3–N), 5.94 (s, 2H, C–CH═C), 7.06 (d, 2H, J = 6.8 Hz, Ar-H), 7.15 (t, 1H, J = 7.6 Hz, Ar-H), 7.20 (t, 1H, J = 7.6 Hz, Ar-H), 7.27–7.39 (m, 4H, Ar-H). ESI-MS, m/z: 510.3 $[M + H]^+$.

*2.7.3.4. Dye **3d**.* Syntheses and purification of **3d** were the same as that of **3b** and blue-purple crystal (254 mg) was collected. However, analyzing the MS and ^{1}H NMR of the compound, we found the crystal was not our target compound **3d** but **3e**. The reason was discussed in the part 3. The yield of dye **3e** was 60%. ^{1}H NMR (400 MHz, $CDCl_3$, ppm): δ1.78 (s, 12H, C(CH_3)$_2$), 3.59 (s, 6H, CH_3–N), 5.93 (s, 2H, C–CH═C), 7.03 (d, 2H, J = 7.6 Hz, Ar-H), 7.15 (t, 2H, J = 7.6 Hz, Ar-H), 7.35 (m, 4H, Ar-H). ESI-MS, m/z: 425.2 $[M + H]^+$.

3. Results and discussion

3.1. Synthesis

The novel dyes were synthesized by condensation of squaric acid and two equivalents of 3*H*-indolium salts in *n*-butanol-toluene-pyridine mixed solvent. In the cases of **2a** (*N*-ethyl-2,3,3-trimethyl-3*H*-indolium) and **2b** (*N*-(*N*′*N*′-diethylcarbamoyl)methyl-2,3,3-trimethyl-3*H*-indolium), the reactions provided moderate yields of the respective dyes (**3a**, **3b**). However, for the reactions of **2c** (*N*-(*N*′-propylcarbamoyl) methyl-2,3,3-trimethyl-3*H*-indolium) and **2d** (*N*-ethoxycarbonyl)methyl-2,3,3-trimethyl-3*H*-indolium), the expected products (**3c** and **3d**) were not obtained. The separated products were unsymmetrical **3c$_1$** and symmetrical **3e**, respectively, where *N*-carbamoylmethyl or *N*-ethoxycabonylmethyl groups were changed to *N*-methyl substituent.

The reason might be that the methylene linking nitrogen cation (N^+) and carbonyl group are so reactive, just like the cases in literatures [20,21], that in basic and heating conditions, *N*-carbamoylmethyl (**2c**) or *N*-ethoxycabonylmethyl (**2d**) groups on 2,3,3-trimethyl-3*H*-indolium are easy to be converted into *N*-methyl indolium(Fig. 5).

The electron-withdrawing abilities of the carbonyl groups of **2b**, **2c** and **2d** are in an order of **2d** > **2c** > **2b**, which correlates with the yields of dyes: **3d** < **3c$_1$** < **3b**. In order to confirm the mechanism, **2d** (2 mmol) was treated 2 h in the same conditions as those of synthesizing dyes, where a colorless transparent crystal with green fluorescence was obtained. The crystal was confirmed to be the *N*-methyl-2,3,3-trimethyl-3*H*-indolium (**2e**) by mass spectrometry and ^{1}H NMR spectroscopy.

3.2. Spectral properties

The spectra data of the dyes in different solvents are listed in Table 1. In same organic solvents, the spectral shapes of the dyes are almost the same. Typical absorption and emission spectra of the dyes in organic solvents are illustrated in Fig. 6. In aqueous solution,

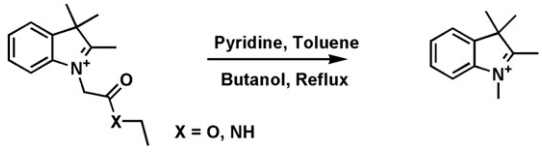

Fig. 5. Decomposition of *N*-carbonylmethyl-2,3,3-trimethyl-3*H*-indolium.

Table 1
Spectral data of the dyes in different solvents.

dye	solvent	Absorption/ Emission (nm)	Stokes Shift (nm)	ε (× 10^5 mol^{-1} cm^{-1} L)	ϕ[a]
3a	Chloroform	633/643	10	2.17	0.19
	Acetone	632/647	15	2.42	0.12
	DMSO	642/652	10	2.28	0.23
	Methanol	627/636	9	2.43	0.072
	Water	621/632	11	0.5	0.005
3b	Chloroform	633/643	10	1.79	0.16
	Acetone	633/645	12	2.06	0.16
	DMSO	643/653	10	1.99	0.28
	Methanol	627/636	9	2.27	0.16
	Water	622/633	11	1.57	0.022
3b$_1$	Chloroform	633/642	9	2.25	0.11
	Acetone	632/641	9	2.53	0.12
	DMSO	642/653	11	2.34	0.17
	Methanol	626/635	9	2.42	0.076
	Water	620/631	11	1.20	0.013
3c$_1$	Chloroform	637/647	10	2.53	0.20
	Acetone	632/642	10	2.85	0.13
	DMSO	638/653	15	2.70	0.25
	Methanol	626/636	10	2.78	0.078
	Water	619/631	12	0.96	0.011

[a] : λex: 600 nm, error ca. ±10%.

however, the spectra of the dyes are much different. In order to facilitate comparisons of the spectra in water and acetone, the spectra in acetone are normalized relative to corresponding spectra in water. As shown in Fig. 6, the absorption spectrum of **3a** becomes broad with two round peaks at 550 nm and 675 nm and the spectra have several nanometers blue-shift comparing to those obtained in organic solvents. The peaks are characteristic of assembly of cyanine dyes into non-covalent dimers and higher aggregations [22,23]. In the case of dye **3b**, the absorption spectrum in water has no obvious round peak except 10–20 nm blue-shift. The shapes of the spectra are similar with those obtained in organic solvents. The aggregation of **3a** leads to the fluorescence intensity of only one eighth of that of **3b** (Fig. 6) and ϵ value 30% of that of **3b** in water (Table 1).

3.3. Aggregation

The aggregation of cyanine dyes is extremely favored by strong attractive dispersion forces derived from the high polarizability of

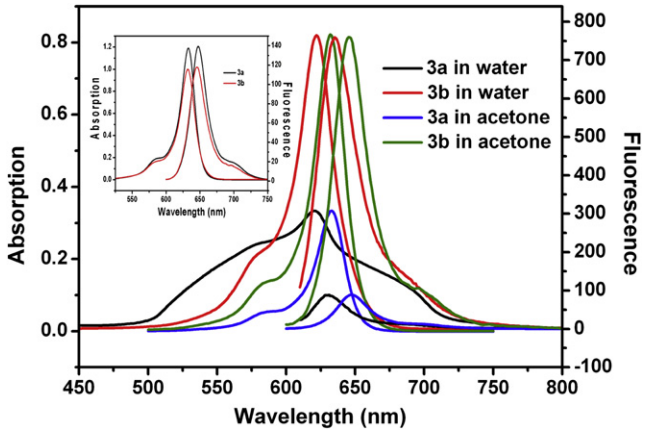

Fig. 6. Comparisons on the spectra of 5 μM dye 3a and 3b in water and acetone. 3a in water (black lines), 3b in water (red lines), 3a in acetone (blue lines, normalized), 3b in acetone (green lines, normalized), inset: the spectra of 3a and 3b in acetone before being normalized.

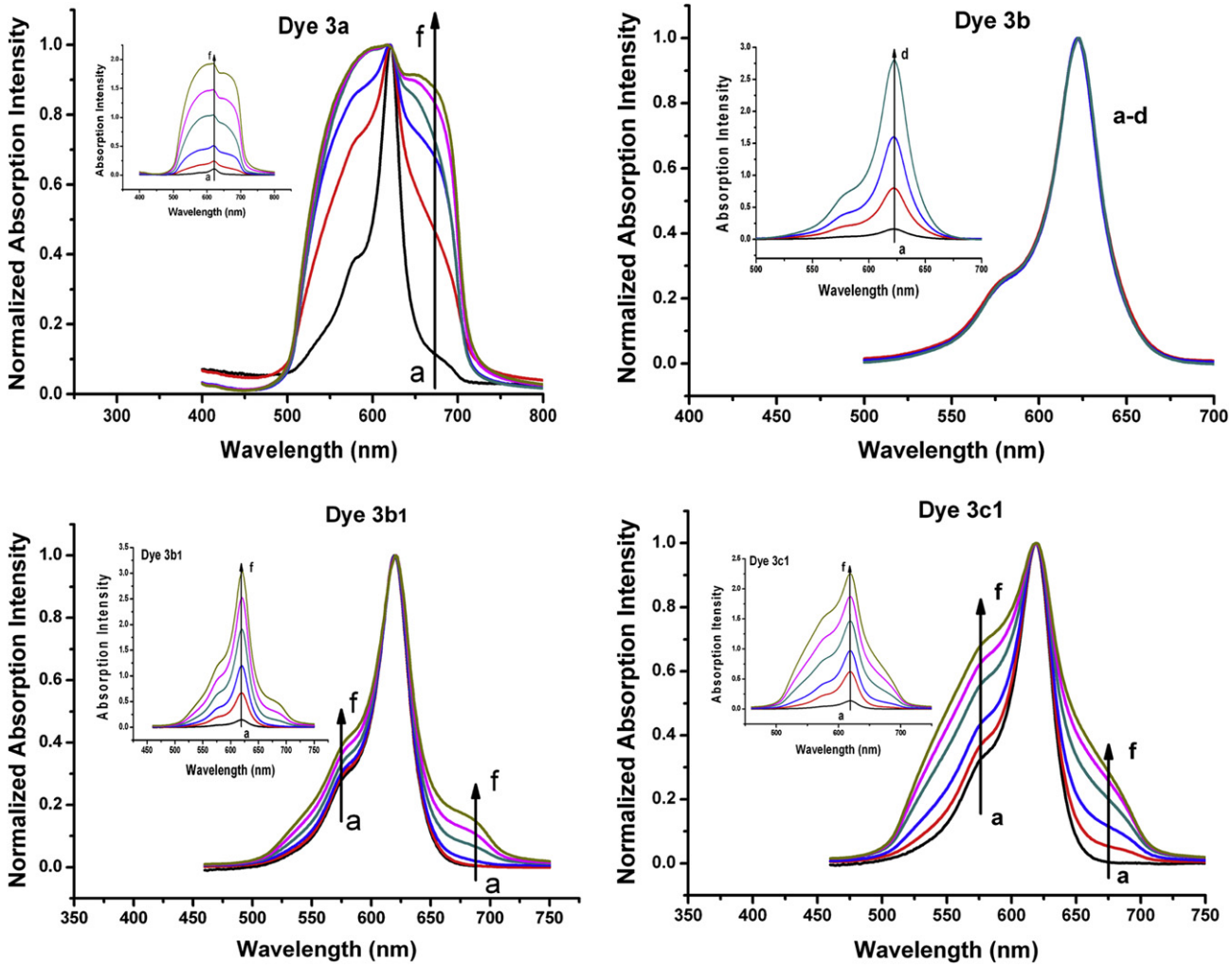

Fig. 7. Normalized absorption spectra of dye 3a, 3b, 3b1 and 3c1 in different concentrations in water. a–f: 1 (black line), 5 (red line), 10 (blue line), 20 (dark cyan line), 30 (magenta line) and 40 μM (dark yellow line), inset: absorption spectra before being normalized.

the chromophoric chain in aqueous solution. Moreover, the high dielectric constant of water facilitates the aggregation process [24–30]. In this paper, the aggregates were detected through recording the absorption spectra of increasing concentration of the dyes in water in order to facilitate the formation of aggregates. Normalized absorption spectra of dye **3a**, **3b**, **3b1** and **3c1** are shown in Fig. 7. When the concentration of **3a** in water is increased, the absorption band becomes broad at the expense of a rise of relative intensity of the short-wavelength shoulder at 580 nm and of the long-wavelength part of the spectrum (675 nm), which reveals the formation of aggregates [23]. In the same manner, dye **3b1** and **3c1** form lower aggregations from their normalized absorption spectra. Nevertheless, the normalized absorption spectra of dye **3b** overlap completely which implies that few aggregations have formed.

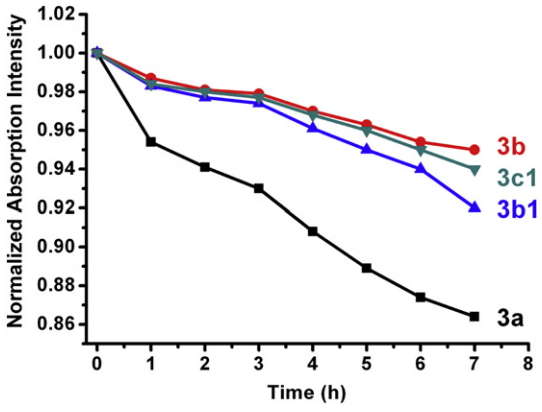

Fig. 8. Comparisons on the photo-stability of the dyes in CH_3CN.

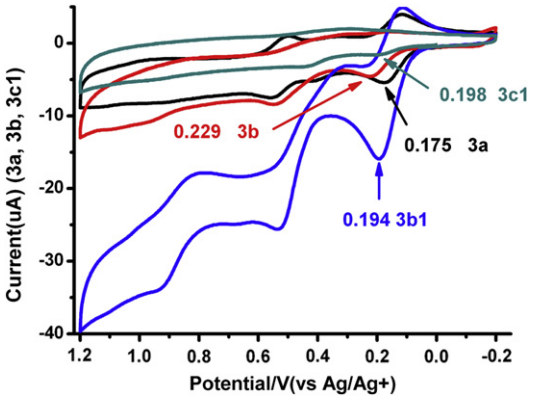

Fig. 9. The redox spectra of dye 3a (black line), 3b (red line), 3b1 (blue line) and 3c1 (dark cyan line) with scan rate of 100 mV/s and the concentrations of the dyes were 10^{-3} M in CH_3CN.

In the other hand, the loss of monomer absorption intensity for 20 μM dyes resulted from the aggregations relative to 1 μM dyes was 51.9%, 12.5%, 33.5% and 45.5% for **3a**, **3b**, **3b1** and **3c1**, respectively.

All the differences suggest that the introduction of the carbamoylmethyl group can inhibit the aggregation of the squarylium dyes in water which is beneficial to their application in aqueous media, and the dialkylcarbamoylmethyl group can decrease the aggregations of the dyes more remarkably than the monoalkylcarbamoylmethyl one.

3.4. Photostability

The results of photo-stability of the dyes are shown in Fig. 8. After irradiation by I/W lamp for 7 h, the absorption intensities of

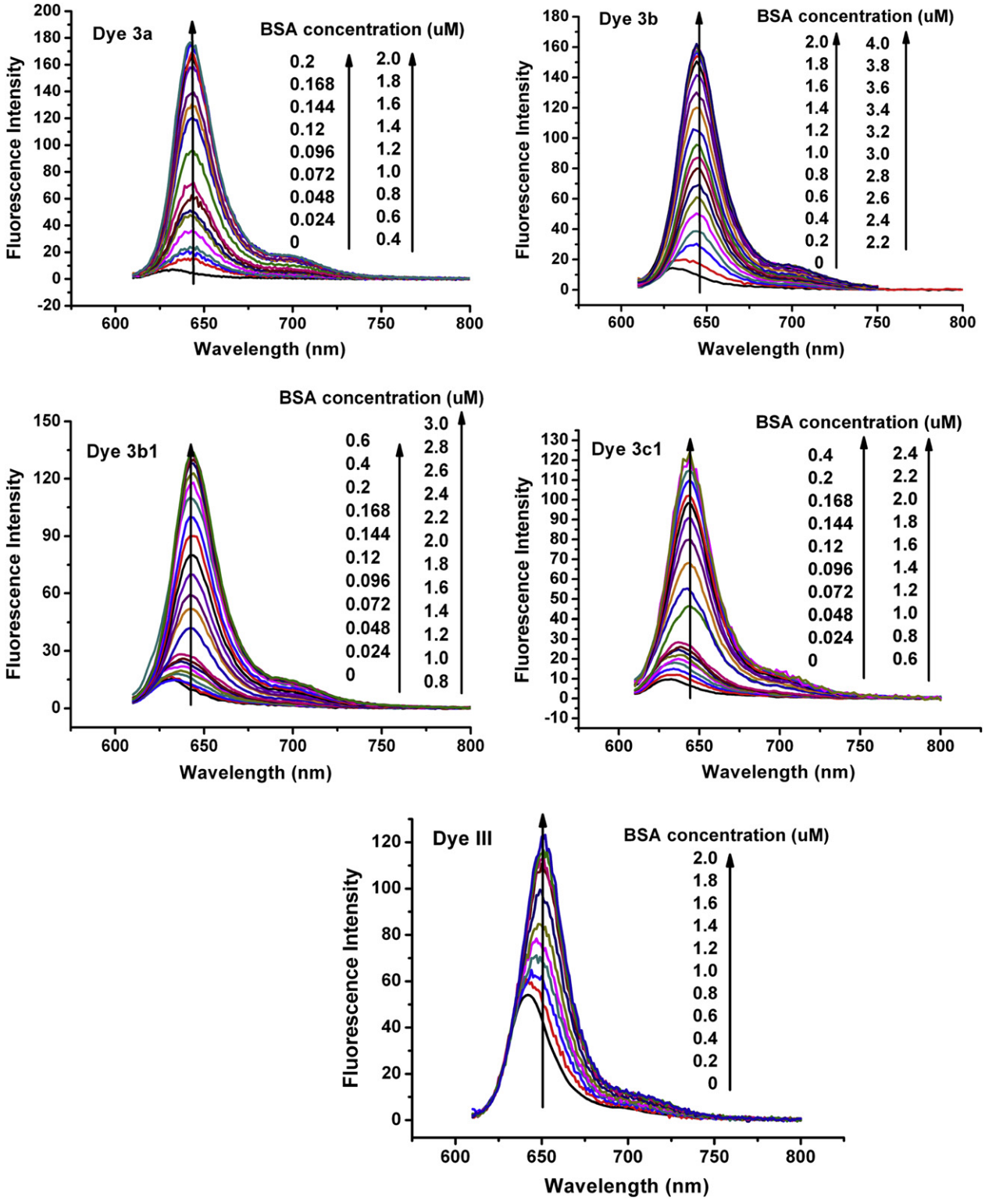

Fig. 10. Fluorescence spectra of 2 μM dye 3a, 3b, 3b1, 3c1 and III associated with BSA in pH = 7.0 PBS at room temperature.

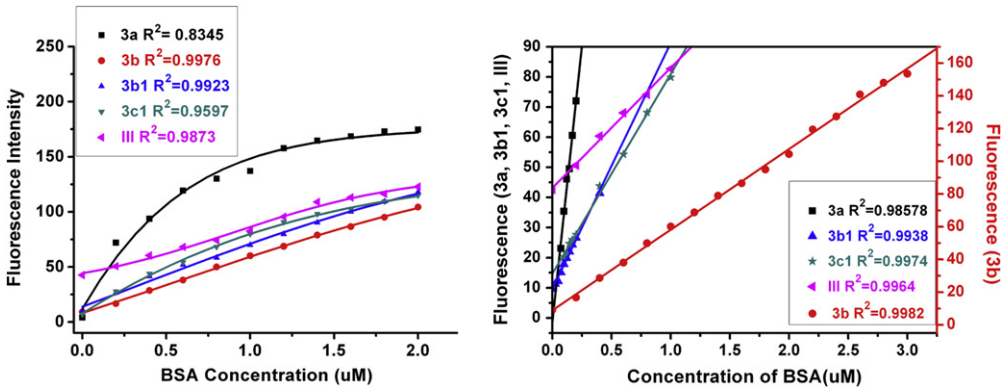

Fig. 11. left: Sigmoidal fit of the fluorescence intensity of 2 μM dye–BSA at 645 nm (dye III at 650 nm) and BSA concentrations in pH = 7.0 PBS, inset text: the errors of linear fit; right: The best linear relationship range for each dye.

3a, **3b**, **3b$_1$** and **3c$_1$** decrease to 86%, 95%, 92% and 94% from 100% respectively. The photo-stabilities of the novel dyes with *N*-carbamoylmethyl group are better than that of the well-known dye **3a**.

The decomposition pathway of cyanine dyes had been depicted in the literature. Singlet oxygen was an important oxidation species which could be produced *in situ* by irradiation of dyes [31–33] and bleach cyanine dyes through destroying the conjugation of the dyes. On the other hand, it was reported that quenching of singlet oxygen by cyanine dyes decreased as the oxidation potential of the dye increased [34].

As seen in Fig. 9, the redox spectra of dye **3a**, **3b, 3b$_1$** and **3c$_1$** were examined. The first oxidation potentials of **3b, 3b$_1$** and **3c$_1$** are more positive than that of **3a** which is likely due to the electron-withdrawing *N*-carbamoylmethyl substituent. This suggests that these new dyes should be less susceptible to reaction with singlet oxygen, i.e. the oxidation of the new dyes by singlet oxygen will not be easy to carry out. The other reason for this might be that the carbamoylmethyl groups are larger and sterically hinder attack by both singlet oxygen and other oxidation species which contribute to the photo-fading of the dyes.

3.5. Dye–BSA association

It was suggested that these squarylium dyes occupy a common hydrophobic binding site on protein to form dye–protein complex [10], which may enhance the fluorescence of the dyes and be used for the determination of proteins. The fluorescence spectra of dye **3a**, **3b**, **3b1**, **3c1** and **III** (Y = COOH) associated with different concentration of BSA are shown in Fig. 10. The fluorescence intensities of the dyes increased by adding BSA in pH 7.0 PBS as expected.

The fluorescence of the dyes at 645 nm (dye III at 650 nm) is plotted as a function of BSA concentration (Fig. 11 left). Better linear relationship ($r^2 = 0.9976$) between the fluorescence intensity of dye **3b** and the BSA concentration (0–2 μM) can be obtained than those of the other dyes. The aggregation of dyes and nonlinear and sigmoidal calibration curves are two of the disadvantages for the reagents used for the fluorescence spectrometry and for the other analytical methods during the protein measurement [35]. The introduction of *N*-carbamoylmethyl group into squarylium dyes can provide a way to resolve these problems.

The better linear range for each dye was studied and the data are presented as following: 0.072–0.2 μM for 3a, 0.2–3 μM for 3b, 0.024–0.4 μM for 3b1, 0.096–1 μM for 3c1 and 0.2–1 for III, respectively (Fig. 11 right). The sensitivity of dye **3b** is lower than other dyes because of the lower fluorescence enhancement. However, the linear range is the largest (0–3 μM). Contrarily, dye **3a** is very sensitive in low concentrations of BSA, while the linear range is very small (0.072–0.2 μM). The fluorescence backgrounds of these dyes are very low except dye III which is the most soluble in water. Fig. 11 shows the relationships on larger scale. It illustrates that less water soluble dye (**3a**) has high fluorescent response with small linear range in lower BSA concentrations, while higher water-solubility dyes (**3b** and **III**) have lower fluorescent response with wider linear range in higher concentration of BSA.

Three different pH buffer solution (pH = 5 Na_2HPO_4/citric acid, pH = 7 PBS and pH = 9 borax) were used to study the effect of pH on the dye–BSA association. Fig. 12 indicates the pH have different effects. In the cases of dye **3a** and **3b**, the pH affects mostly the state of BSA. At pH 5, BSA may be protonated so that the dye–BSA associations of dye **3a** and **3b** are weakened and the fluorescence intensity become lower. At pH 7.0 and pH 9.0, the interactions are

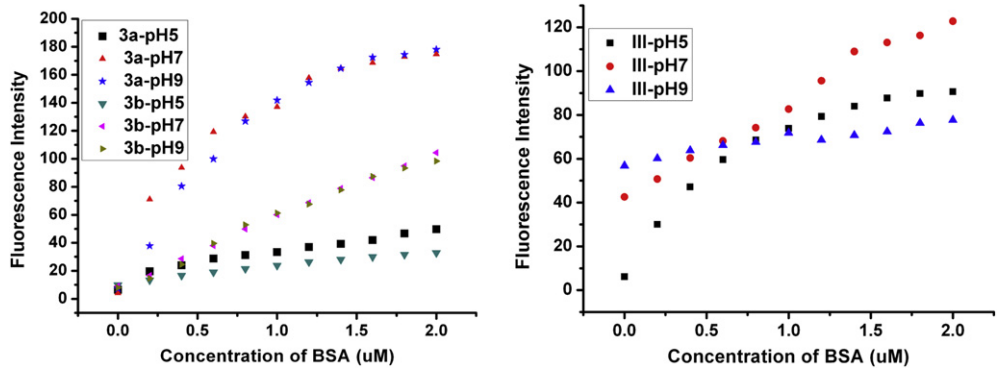

Fig. 12. Plot of the fluorescence of 2 μM dye–BSA at 645 nm (dye III at 650 nm) in pH = 5, 7, 9 buffer solutions as a function of BSA concentrations (0–2 μM).

much similar and show high fluorescent enhancement. In the case of dye III ($Y = CO_2H$), the 3 pH have the different effects on dye–BSA interaction. At pH 9, the deprotonation of the dye carboxyl group alters the electric property, increases the water-solubility of the dye and decreases the trend of the association with BSA so that the fluorescence enhancement becomes smaller.

4. Conclusion

In summary, we have synthesized new squaraine dyes containing *N*- alkylcarbamoylmethyl-2,3,3-trimethyl-3*H*-indolium and tested their properties such as fluorescence, aggregation, photo-stability and fluorescent response to BSA. The results showed that the introduction of alkylcarbamoylmethyl group decrease the aggregations and increase the photo-stability and fluorescence quantum yields of the dyes in water. Among the dyes, **3b** with two 1-(*N*', *N*'-diethylcarbamoyl)methyl- 2,3,3-trimethyl-3*H*-indolium groups has good fluorescence quantum yield, high photo-stability and excellent linear relationship between fluorescent intensity and BSA concentration. The pH of the buffer solution for testing has dissimilar effect to the different dye–BSA associations. These positive results arising from the introduction of alkylcarbamoylmethyl group would be worthwhile to design new squaraine dyes with powerful functions for their wide applications.

Acknowledgements

This work was supported by NSF of China (20706008, 20725621 and 20872012), National Basic Research Program of China (2009CB724706), Ministry of Education of China (Program for Changjiang Scholars and Innovative Research Team in University, IRT0711 and Cultivation Fund of the Key Scientific and Technical Innovation Project, 707016).

References

[1] Hyodo Yutaka, Nakazumi Hiroyuki, Yagi Shigeyuki. Synthesis and light absorption /emission properties of novel squarylium dimers bearing a ferrocene spacer. Dyes and Pigments 2002;54:163–71.
[2] Law KY. Organic photoconductive materials: recent trends and developments. Chemical Reviews 1993;93. 449–406.
[3] Kim SH, Kim JH, Cui JZ, Gal YS, Jin SH, Koh K. Absorption spectra, aggregation and photofading behaviour of near-infrared absorbing squarylium dyes containing perimidine moiety. Dyes and Pigments 2002;55:1–7.
[4] Law KY, Court BF. Squaraine chemistry: effect of synthesis on the morphological and xerographic properties of photoconductive squaraines. Journal of Imaging Science 1987;31(4):172–7.
[5] Alex S, Santhosh U, Das S. Dye sensitization of nanocrystalline TiO2: enhanced efficiency of unsymmetrical versus symmetrical squaraine dyes. Journal of Photochemistry and Photobiology A: Chemistry 2005;172:63–71.
[6] Fabian J. Near-infrared absorbing dyes. Chemical Reviews 1992;92:1197–226.
[7] Patonay G, Salon J, Sowell J, Strekowski L. Noncovalent labeling of biomolecules with red and near-infrared dyes. Molecules 2004;9:40–9.
[8] Nizomov N, Ismailov ZF, Nizamova SN, Salakhitdinova MK, Tatarets AL, Patsenker LD, et al. Spectral-luminescent study of interaction of squaraine dyes with biological substances. Journal of Molecular Structure 2006;788:36–42.
[9] Welder F, Paul B, Nakazumi H, Yagi S, Colyer CL. Symmetric and asymmetric squarylium dyes as noncovalent protein labels: a study by fluorimetry and capillary electrophoresis. Journal of Chromatography B 2003;793:93–105.
[10] Meadows F, Narayanan N, Patonay G. Determination of protein–dye association by near infrared fluorescence-detected circular dichroism. Talanta 2000; 50:1149–55.
[11] Kim SH, Hwang SH. Synthesis and photostability of functional squarylium dyes. Dyes and Pigments 1997;35(2):111–21.
[12] Kim SH, Hwang SH, Kim NK, Kim JW, Yoon CM, Keum SR. Aggregation and photofading behaviour of unsymmetrical squarylium dyes containing a quinolylidene moiety. Journal of Society of Dyers and Colourists 2000;116: 126–31.
[13] Song B, Zhang Q, Ma WH, Peng XJ, Fu XM, Wang BS. The synthesis and photostability of novel squarylium indocyanine dyes. Dyes and Pigments 2009;82:396–400.
[14] Frangioni JV. In vivo near-infrared fluorescence imaging. Current Opinion in Chemical Biology 2003;7:626–34.
[15] Reddington MV. New glycoconjugated cyanine dyes as fluorescent labeling reagents. Journal of Chemistry Society, Perkin Translation 1998;1:143–7.
[16] Deligeorgiev T, Vasilev A, Drexhage KH. Synthesis of novel cyanine dyes containing carbamoylethyl component-Noncovalent labels for nucleic acids detection. Dyes and Pigments 2007;74:320–8.
[17] Karstens T, Kobs K. Rhodamine B and rhodamine 101 as reference substances for fluorescence quantum yield measurements. The Journal of Physical Chemistry 1980;84:1871–2.
[18] Velapoldi RA, TÖnnesen HH. Corrected emission spectra and quantum yields for a series of fluorescent compounds in the visible spectral region. Journal of Fluorescence 2004;14(4):465–72.
[19] Ock K, Jang G, Roh Y, Kim S, Kim J, Koh K. Optical detection of Cu^{2+} ion using a SQ-dye containing polymeric thin-film on Au surface. Microchemical Journal 2001;70:301–5.
[20] Laird T, Williams H. Phstolysis and rearrangement reactions of a-bromophenacyl oniurn salts. Journal of the Chemical Society C: Organic 1971:3467–71.
[21] Roberts RM, Edwards MB. Acetoacetic ester-type cleavage by aniline. Journal of the American Chemical Society 1950;72:5537–9.
[22] Chen H, Farahat MS, Law KY, Whitten DG. Aggregation of surfactant squaraine dyes in aqueous solution and microheterogeneous media: correlation of aggregation behavior with molecular structure. Journal of the American Chemical Society 1996;118:2584–94.
[23] Tatikolov AS, Costa SMB. Photophysical and aggregation properties of a long-chain squarylium indocyanine dye. Journal of Photochemistry and Photobiology A: Chemistry 2001;140:147–56.
[24] Chibisov AK, Zakharova GV, Gorner H. Photoprocesses of thiamono- methinecyanine monomers and dimers. Physical Chemistry Chemical Physics 2001;3:44–9.
[25] Sabate R, Gallardo M, Maza A, Estelrich J. A spectroscopy study of the interaction of pinacyanol with *n*-dodecyltrimethylammonium bromide micelles. Langmuir 2001;17:6433–7.
[26] Sabate R, Estelrich J. Determination of micellar microenvironment of pinacyanol by visible spectroscopy. Journal of Physical Chemistry B 2003;107: 4137–42.
[27] Sabate R, Estelrich J. Determination of the dimerization constant of pinacyanol: role of the thermochromic effect. Spectrochimica Acta Part A 2008;70: 471–6.
[28] Law KY, Chen CC. Squaraine chemistry. Effect of orientation on the aggregation of surfactant squaraines in langmuir-biodgett films. Journal of Physical Chemistry 1989;93:2533–8.
[29] Grynyov RS, Sorokin AV, Guralchuk GY, Yefimova SL, Borovoy IA, Malyukin YA. Squaraine dye as an exciton trap for cyanine J-aggregates in a solution. Journal of Physical Chemistry C 2008;112:20458–62.
[30] Chowdhury A, Sebastian WH, Bangal PR, Raheem I, Peteanu LA. Characterization of chiral H and J aggregates of cyanine dyes formed by DNA templating using stark and fluorescence spectroscopies. Journal of Physical Chemistry B 2001;105:12196–201.
[31] Kanony C, Akerman B, Tuite E. Photobleaching of asymmetric cyanines used for fluorescence imaging of single DNA molecules. Journal of the American Chemical Society 2001;123:7985–95.
[32] Chen P, Li J, Qian ZG, Zheng DS, Okazaki T, Hayami M. Study on the photooxidation of a near-infrared-absorbing benzothiazolone cyanine dye. Dyes and Pigments 1998;37(3):213–22.
[33] Renikuntla BR, Rose HC, Eldo J, Waggoner AS, Armitage BA. Improved photostability and fluorescence properties through polyfluorination of a cyanine dye. Organic Letter 2004;6(6):909–12.
[34] Kanofsky JR, Sima PD. Structural and environmental requirements for quenching of singlet oxygen by cyanine dyes. Photochemistry and Photobiology 2000;71:361–8.
[35] Suzuki Y, Yokoyama K. Design and synthesis of intramolecular charge transfer-based fluorescent reagents for the highly-sensitive detection of proteins. Journal of the American Chemical Society 2005;127:17799–802.